Finite Element Modeling of the Pulmonary Autograft at Systemic Pressure before Remodeling

Article *in* The Journal of heart valve disease · January 2011

Source: PubMed

7 authors, including:

Choon-Sik Jhun
Pennsylvania State University
41 PUBLICATIONS **480** CITATIONS

SEE PROFILE

Stephanie Yaung
Massachusetts Institute of Technology
96 PUBLICATIONS **1,454** CITATIONS

SEE PROFILE

Ali Azadani
University of Denver
92 PUBLICATIONS **1,761** CITATIONS

SEE PROFILE

Julius M Guccione
University of California, San Francisco
221 PUBLICATIONS **7,083** CITATIONS

SEE PROFILE

Finite Element Modeling of the Pulmonary Autograft at Systemic Pressure before Remodeling

Peter B. Matthews, Choon-Sik Jhun, Stephanie Yaung, Ali N. Azadani, Julius M. Guccione, Liang Ge, Elaine E. Tseng

Department of Surgery, University of California at San Francisco Medical Center and San Francisco Veterans Affairs Medical Center, San Francisco, CA, USA

Background and aim of the study: **Pulmonary autograft dilatation requiring reoperation is an Achilles' heel of the Ross procedure, as exposure to systemic pressure increases autograft wall stress, which may in turn lead to tissue remodeling and aneurysmal pathology. However, the magnitude of autograft wall stress with the Ross procedure is unknown. The study aim was to develop a realistic finite element (FE) model of the autograft, and to perform simulations at systemic pressure to determine wall stress distribution immediately after the Ross operation.**

Methods: **The porcine pulmonary root geometry was generated from high-resolution microcomputed tomography (microCT) images to create a mesh composed of hexahedral elements. Previously defined constitutive equations were used to describe the regional material properties of the native porcine pulmonary root. The anterior and posterior pulmonary arteries, and each of the pulmonary sinuses, were best described by non-linear, anisotropic Fung strain energy functions, and input individually into the model. Autograft dilatation and wall stress distribution during pulmonary and systemic loading prior to remodeling were determined using explicit FE analysis in LS-DYNA.**

Results: **The autograft was highly compliant in the low-strain region, and the majority of dilation occurred with <30 mmHg of pressurization. During pulmonic loading, a typical inflation/deflation was observed between systole and diastole, but the autograft remained almost completely dilated throughout the cardiac cycle at systemic pressure. Although the systolic blood pressure was 380% greater in the aortic than in the pulmonary position, the peak systolic diameter was increased by only 28%. The maximum principal wall stress increased approximately 10-fold during systole and 25-fold during diastole, and was greater in the sinus than the distal artery for all simulations.**

Conclusion: **Under systemic loading conditions, the pulmonary autograft remained fully dilated and experienced large wall stresses concentrated in the sinus. The future correlation of this model with explanted autografts may lead to an improved understanding of tissue remodeling following the Ross procedure.**

The Journal of Heart Valve Disease 2011;20:45-52

Aortic valve replacement with the pulmonary autograft, though originally implanted via a subcoronary technique, has been most commonly been performed as a full aortic root replacement since the late 1980s (1). However, late failure from autograft dilatation requires reoperation, and this is a critical limitation of the procedure (2-6). Significant autograft dilatation leading to aortic regurgitation or aneurysm formation occurs after biological remodeling when the pulmonary root, which is accustomed to pulmonary pressures, is subjected to systemic pressures within the aorta. Biologic remodeling involves reduced elastin and elastin fragmentation in the media of the wall, increased collagen and fibrosis, and hypertrophy of the smooth muscle (7). Remodeling is thought to be triggered by increases in autograft wall stress from pulmonary to systemic pressure; however, the autograft wall stress that occurs on an initial exposure to aortic pressures is unknown. Wall stress may be determined by computational simulations (8) of the auto-

Presented in part at the 94th Annual Clinical Congress of the American College of Surgeons, Owen H. Wangensteen Surgical Forum, San Francisco, CA, 14th October 2008, and as a poster at the Fifth Biennial Meeting of the Society for Heart Valve Disease, 27th-30th June 2009, Berlin, Germany

Address for correspondence:
Elaine E. Tseng MD, UCSF Medical Center, Division of Cardiothoracic Surgery, 500 Parnassus Avenue, Suite W405, Box 0118, San Francisco, California 94143-0118, USA
e-mail: elaine.tseng@ucsfmedctr.org

J Heart Valve Dis
Vol. 20. No. 1
January 2011

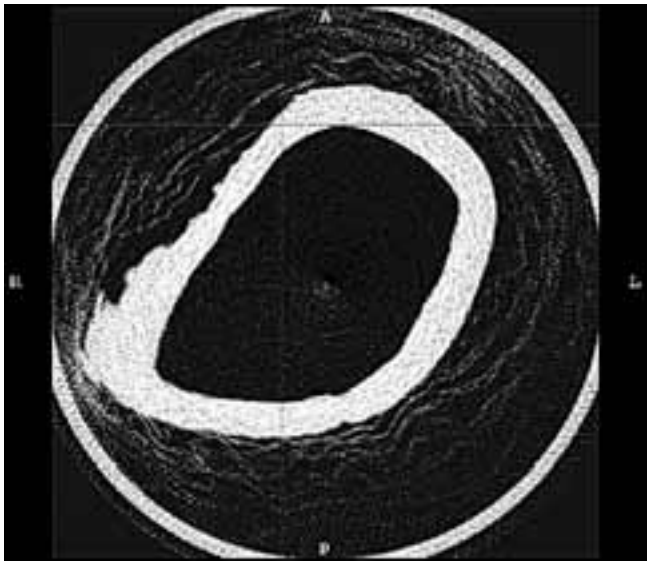

Figure 1: Cross-sectional axial slice of a microCT image of a pulmonary autograft at the level of the sinotubular junction.

graft during the cardiac cycle under pulmonary and systemic loading conditions. Computational modeling is a valuable tool for evaluating the mechanical load on the autograft at the time of implantation, and can potentially assist the surgeons to tailor their implantation method (9,10). Constitutive equations of regional material properties of the pulmonary root - anterior and posterior pulmonary artery (PA), and each of the three sinuses - using biaxial tensile testing within and beyond physiologic range of strain have been previously defined (11). These strain energy functions, which describe regions of the autograft mechanically, may be used as input parameters for computational models (11,12). In the present study, a finite element (FE) model of the porcine pulmonary autograft was created from realistic geometry, and the material properties for individual regions of the root were determined experimentally. The model was loaded with pulmonary and systemic pressures to quantify increases in dilation and wall stress in the autograft that occur initially after the Ross procedure, prior to remodeling.

Materials and methods

Pulmonary root mesh generation

The autograft model was generated from the realistic anatomic geometry of the porcine pulmonary root. The porcine model was chosen as it has a similar cardiovascular anatomy to that of humans; moreover, porcine - but not human - regional material properties have previously been determined (12,13). The acquisition of fresh human tissue from autopsy for mechanical testing within 24 h is difficult; hence, a fresh porcine heart was obtained at a local abattoir on the morning of harvest for dissection.

At the pulmonary annulus a small ring of ventricular muscle surrounding the valve was cut, and the pulmonary root removed in its entirety. Distally, the PA was cut approximately 2 cm below the bifurcation, after which the root was washed with isotonic saline and placed upright within a sample container for fixation with 10% dilute formalin. The lumen of the root was packed with small Styrofoam beads in order to maintain a cylindrical shape during fixation; care was taken to prevent dilation of the root during preparation, so as to maintain a stress-free geometry. The sample was fixed for 24 h, after which the Styrofoam beads were removed and the pulmonary root was imaged using a desktop cone-beam micro-computed tomography scanner (microCT-40; Scanco Medical AG, Baseldorf, Switzerland).

High-resolution DICOM (Digital Imaging and COmmunications in Medicine) radiologic images of the pulmonary root - the pulmonary sinuses, sinotubular junction (STJ), and PA (voxel size 76 × 76 × 76 μm; Fig. 1) were imported into ITK-SNAP (www.itksnap.org), an open-source image segmentation software (14). The images were filtered using an intensity threshold to separate the geometry of the autograft from background. A surface mesh of the outer autograft wall and inner lumen was created with Rapidform XOR (INUS Technology, Inc., Sunnyvale CA, USA) (Fig. 2a), excluding the pulmonary valve leaflets. The autograft wall, the space between the surfaces, was then filled with hexahedral elements (TrueGrid; XYZ Scientific, Inc., Livermore, CA, USA), thus creating a volume mesh of accurate size and thickness at zero stress. The total number of elements used was approximately 10^5.

Finite element analysis

The autograft model was assigned the material properties of the native porcine pulmonary root that have been determined previously (11,12). These properties were determined on fresh (not fixed) pulmonary roots obtained within 24 h of harvest, to determine the mechanical behavior. The mesh was divided into five regions corresponding to the anterior and posterior PA and the three sinuses. All regions were described with an anisotropic, non-linear constitutive equation with the following strain energy function:

$$W = \frac{C}{2}\left\{\exp\left[b_f E_{11}^2 + b_t\left(E_{22}^2 + E_{33}^2 + E_{23}^2 + E_{32}^2\right)\right] - 1\right\}$$

where E_{11} is the circumferential strain, E_{22} is the longitudinal strain, E_{33} is the radial strain, and E_{23} is the shear strain in the transverse plane. Parameters of this function were unique for each of the five regions, and

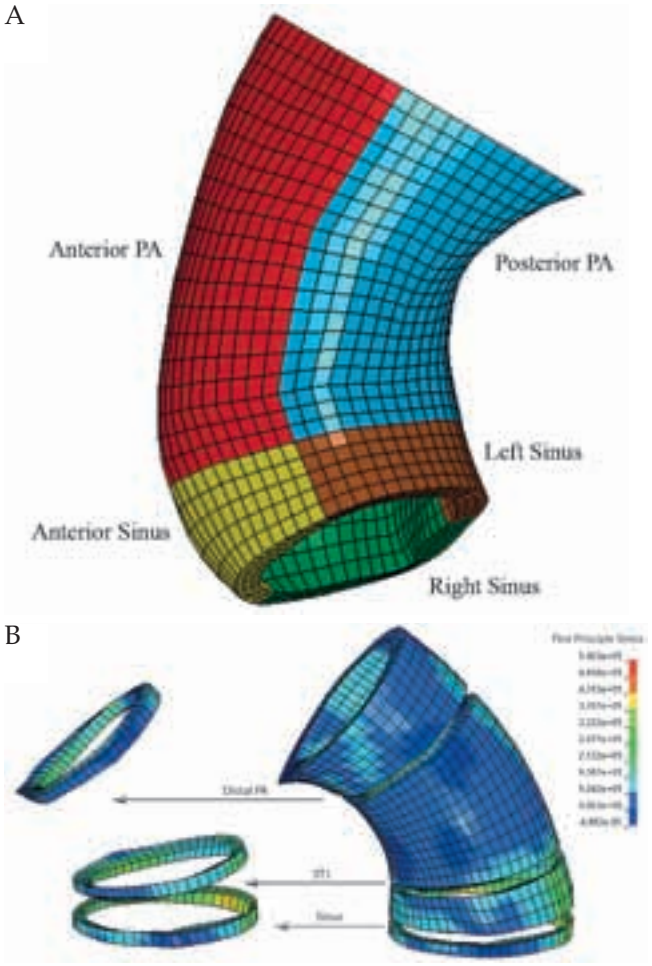

Figure 2: (a) Surface mesh of pulmonary autograft created in RapidForm from microCT images. (b) Wall stress on the autograft mesh displayed with rings at the sinuses, sinotubular junction (STJ), and pulmonary artery (PA).

determined from biaxial stretch testing.

The commercial explicit FE solver LS-DYNA (LSTC, Inc., Livermore, CA, USA) was used for modeling and analysis. An arterial pressure was uniformly applied to the luminal surface of the mesh, with a loading curve representative of human physiology. In order to quantify changes in autograft wall stress and dilation associated with the Ross operation, two simulations were conducted: at pulmonary pressure (25/8 mmHg) and aortic pressure (120/80 mmHg). In both cases, systole was 38% of the cardiac cycle. The geometry of the mesh was taken from an unpressurized root, but dilation and wall stress on the autograft were relevant between diastolic and systolic pressures. Therefore, the model was first given a ramp load from 0 mmHg to systolic pressure (120 mmHg for aortic, 25 mmHg for pulmonary) over a period of 100 ms, followed by relaxation to diastolic pressure (80 mmHg for aortic, 8 mmHg for pulmonary) over an additional 100 ms to reach diastole. As the mesh geometry represented the configuration at 0 mmHg, this ramp loading method to systole removed any unrealistic inertial forces on the autograft and improved the numerical stability during data collection. Simulation of the cardiac cycle was then performed by applying a loading curve from diastole to systole (80-120 mmHg for aortic, 8-25 mmHg for pulmonary) over 300 ms, representing systolic ejection through the autograft, and a 500 ms relaxation to diastole (80 mmHg for aortic, 8 mmHg for pulmonary). A displacement boundary condition was applied at the annulus of the model which constrained movement in the longitudinal axis, but allowed dilation. Additionally, a single node on the annulus was fixed in all three axes, preventing rigid body movement of the mesh. All other elements were unconstrained.

Post-processing and data analysis

The simulation results were examined at slices along three regions of the autograft: sinus (at maximum sinus diameter), STJ, and distal PA. Each slice was isolated as a cross-sectional ring of elements, and each ring was a group of elements, aligned circumferentially, extending full thickness through the autograft (Fig. 2b). The locations of the cross-sections were chosen to correspond with positions at which the autograft diameter had been measured clinically, using echocardiography. With this method the model could be validated by comparing the calculated diameter with autograft diameters of patients reported elsewhere.

To measure the size of the autograft, the position of two elements in the ring that had the greatest diameter during peak systole were chosen. The location of these elements was tracked through the duration of simulation, and their distances at systole and diastole were reported. The first-principles stress was also calculated, using LS-DYNA post-processing software. The stress on all elements of the ring was averaged, and reported at diastole and systole. This method provided measurements of the total load exerted on the autograft at that axial position. All reported values were quoted as mean ± SD.

Results

Dilation

The pulmonary root underwent a large deformation when loaded from 0 mmHg to pulmonary pressures (25 mmHg), based on its non-linear material properties. However, beyond 30 mmHg the stiffness of the pulmonary root tissue increased significantly, and limited further dilation at systemic pressure. The average size of the autograft at end-systole was 25-28 mm diameter at pulmonary pressure, and 30-35 mm at sys-

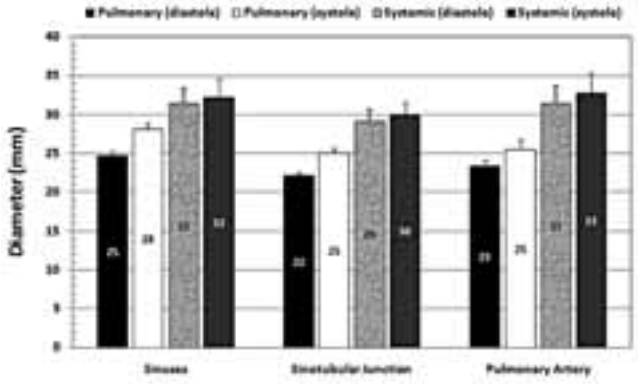

Figure 3: Diameters of each autograft region (sinuses, sinotubular junction, and pulmonary artery) at pulmonary diastolic and systolic pressures and systemic diastolic and systolic pressures.

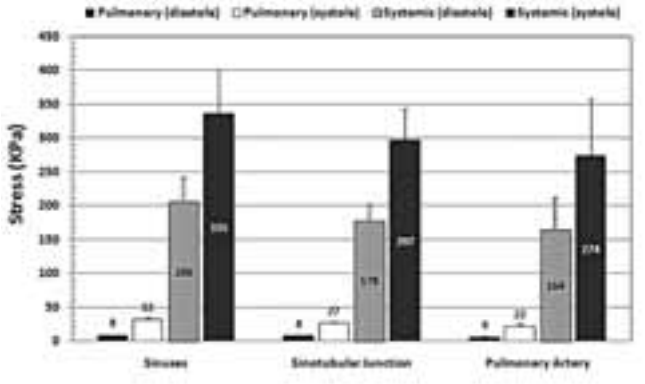

Figure 4: Wall stress of rings in each pulmonary autograft region (sinuses, sinotubular junction, and pulmonary artery) at pulmonary diastolic and systolic pressures and systemic diastolic and systolic pressures.

temic pressure (Table I).

Under pulmonary loading conditions, the root expanded and relaxed through the cardiac cycle. Under systemic loading, however, the autograft remained in the high stiffness region at all times, with minimal relaxation during diastole. At pulmonary pressures, the diameter increased during diastole to systole in the three regions, as shown in Table I. When initially exposed to systemic pressures, as expected the diameter of the pulmonary root increased significantly at each level in both systole and diastole (Fig. 3). However, at each level the change in diameter from diastole to systole (distensibility) at pulmonary pressures was greater than the change in diameter from diastole to systole at systemic pressure. This smaller root expansion during the cardiac cycle at systemic pressures reflected the lack of compliance at high strain. Distensibility of the pulmonary root at physiologic pulmonary pressures during the cardiac cycle was 3.36 mm (13.6%), 2.81 mm (12.7%), and 2.08 mm (8.9%) at the sinuses, STJ, and PA, respectively; in contrast, the distensibility was reduced to 0.81 mm (2.6%), 0.75 mm (2.6%), and 1.31 mm (4.2%), respectively, for these regions under systemic loading conditions.

Wall stress

During both pulmonary and systemic loading conditions, the average first-principles wall stress was greatest at end-systole in all regions. The average regional wall stress with pulmonary loading conditions increased, as expected (from diastole to systole), from 8.28 ± 0.49 to 31.84 ± 3.18 kPa, from 7.70 ± 0.49 to 27.14 ± 2.08 kPa, and from 5.84 ± 1.21 to 21.64 ± 5.31 kPa in the sinuses, STJ, and PA, respectively (Fig. 4). Similarly, the average regional wall stress was increased (from diastole to systole) with systemic loading pressures from 205.96 ± 35.93 to 335.26 ± 65.60 kPa, from 178.39 ± 23.32 to 297.10 ± 46.19 kPa, and from 164.15 ± 47.99 to 274.33 ± 84.10 kPa in the sinuses, STJ, and PA, respectively (Fig. 4). In each region, the average wall stress at systemic pressure was approximately 10-fold greater than the autograft wall stress at pulmonary pressures. At systemic pressures, the wall stress in the sinuses was greater than that in the PA. Overall, the change in wall stress from diastole to systole was substantially greater at systemic pressure than at pulmonary pressure (Table II).

Discussion

Using previously determined constitutive equations of regional material properties of the porcine pulmonary root (11,12), a realistic FE model was developed of the pulmonary autograft, and simulations

Table I: Diameters of the autograft regions.

Region	Pulmonary pressures		Systemic pressures	
	8 mmHg	25 mmHg	80 mmHg	120 mmHg
Sinus (mm)	24.70 ± 0.56	28.06 ± 0.89	31.42 ± 2.01	32.23 ± 2.37
STJ (mm)	22.19 ± 0.37	25.00 ± 0.57	29.19 ± 1.47	29.94 ± 1.65
PA (mm)	23.40 ± 0.70	25.48 ± 1.23	31.44 ± 2.39	32.75 ± 2.60

PA: Pulmonary artery; STJ: Sinotubular junction.

Table II: Changes in wall stress from diastole to systole within autograft regions.

Pressure range	Change in wall stress from diastole to systole in:		
	Sinus (kPa)	STJ (kPa)	PA (kPa)
At pulmonary pressure (8-25 mmHg)	23.56	19.44	15.80
At systemic pressure (80-120 mmHg)	129.04	118.71	110.18

PA: Pulmonary artery; STJ: Sinotubular junction.

performed at physiologic pulmonary and systemic pressures prior to remodeling after the Ross procedure. The autograft was seen to dilate greatly from pulmonary to systemic pressure, but then lost its normal root distensibility during the cardiac cycle at systemic pressures. Dilation in the autograft corresponded to a substantial increase in wall stress at systemic pressure, along with large increases in wall stress from diastole to systole at systemic pressures, as opposed to pulmonary pressures.

Echocardiography of pulmonary autograft measurements immediately after the Ross operation

Studies in humans have been conducted to examine the echocardiographic dimensions of the pulmonary autograft immediately after the Ross procedure but prior to biological remodeling, with the results being compared to those obtained with the present porcine autograft simulation. Carr-White et al. (15) showed the autograft annulus to be 26.2 ± 1.9 mm, the sinus to be 37.3 ± 3.8 mm, and STJ to be 29.2 ± 2.2 mm; these data were quite comparable to the presently determined values of 32.2 mm at the sinus and 29.9 mm at the STJ. Similarly, Hokken et al. (2) demonstrated, after cardiopulmonary bypass, an annulus of 27 mm and a sinus of 36 mm, while Kouchoukos et al. (3) reported a sinus of 30.8 mm and an STJ of 26.6 mm within six months of surgery. The results of the present simulation showed that the diameter calculations from this model were well within the range of clinical measurements of human autograft size, and provided an excellent foundation for modification to include autograft remodeling in the future. Indeed, the data cited in the clinical literature provide confidence that the present simulation of the autograft represents a good approximation of the dynamics and stress on the autograft in vivo.

In the present simulation, an examination of autograft dilation from pulmonary diastolic to systemic diastolic pressure revealed that the PA had dilated by 34%, whereas the sinuses had correspondingly dilated by 27%. Similarly, an examination of autograft dilation from pulmonary systolic to systemic systolic pressure revealed that the PA had dilated by 27%, and the sinuses by 15%. Overall, in both diastole and systole, the PA had dilated to a greater extent from pulmonary to systemic pressure than the sinuses, and this was reflective of the greater compliance of the PA than the sinus. A greater initial dilatation by the PA than by the sinus may potentially contribute to aneurysmal formation at the distal portion of the autograft. Consequently, consideration might be given to limiting the length of the PA beyond the STJ used in autograft root replacement, as well as reinforcing the suture line with felt.

Pulmonary autograft dilation at systemic pressure in relation to normal aortic root expansion

Despite substantial autograft dilatation from pulmonary to systemic pressure, at systemic pressure only minimal autograft expansion was demonstrated from diastole to systole, ranging from 2.6% in the sinuses to 4.2% in the PA. In contrast, dynamic in vitro beating porcine hearts showed a 24% radial distensibility of the aortic root from diastole to systole at systemic pressure. The dynamic expansion was two- to six-fold greater than in the static pressurization tests (16). Lockie et al. (17) demonstrated an 11% increase in the sinotubular diameter of human homografts during static pressurization from diastole to systole, which would be expected to be at least 22% in the dynamic setting. Similarly, FE modeling of the homograft aortic root showed that the sinuses dilated by 11.3% during ejection, as well as by an additional 23.1% during isovolumic contraction prior to ejection (18). Overall, the normal aortic root demonstrates a significant expansion during the cardiac cycle, and this is abrogated when the pulmonary autograft is implanted as a root in the aortic position prior to remodeling. Thus, although the pulmonary autograft is greatly expanded in diameter at systemic pressure, it remains fully dilated during the cardiac cycle due to its lack of compliance.

Pulmonary autograft versus normal aortic root wall stresses

The present FE simulations showed that, on average,

the first-principles wall stress of the autograft was increased approximately 10-fold at systole and 25-fold at diastole from pulmonary to systemic pressures. Prior to remodeling, the autograft experiences significant increases in wall stress throughout the cardiac cycle, and at systole this ranged from 274 kPa in the PA to 335 kPa in the sinuses. In contrast, simulations of peak wall stress in the human aortic sinuses were significantly lower, and ranged from 100 to 130 kPa (8). The autograft wall stresses are two- to three-fold greater than the corresponding aortic root wall stresses, and this may trigger remodeling at systemic pressure, with potential for pathologic dilatation. The wall stresses in the sinuses were also found to be greater than in the PA, although whether the magnitude of wall stress difference impacts on the degree of autograft remodeling is unknown.

Currently, little is known of the autograft material properties after remodeling at systemic pressure. The analysis of an explanted pulmonary autograft at four weeks after implantation showed the remodeled autograft to be stiffer than native pulmonary valve, but to be more compliant than the aortic tissue (15). At a systemic pressure of 200 mmHg, the remodeled autograft would expand to a 25% greater diameter than aortic, and a 25% smaller diameter than the pulmonary tissue. Clearly, a better understanding of the remodeled autograft material's properties will be required to accurately determine wall stresses after remodeling.

Autograft remodeling histology

Although Ross originally described autograft valve leaflets as containing a full complement of living cells with the preservation of the endothelium (19), recent microscopic examinations of the pulmonary autograft valve explants have revealed fibrous hyperplasia, increased cell numbers, and also the presence of myofibroblasts that were not seen with normal aortic and pulmonary valves, and are suggested as active remodeling and primary valve-related causes of autograft valve failure (20). An histologic examination of two further explanted autografts demonstrated, within the autograft wall, the disruption of the media focally, with a complete absence of elastin and intimal proliferation with fibrosis (21). In the most extensive histologic series of pulmonary autograft explants, microscopy showed severe aneurysmal degeneration of the wall (7), with the presence of reduced elastin and medial elastin fragmentation, hypertrophied smooth muscle cells, and increased collagen and fibrosis. Intimal thickening was also a common occurrence, while the adventitia showed severe fibrosis. Based on these observations, the remodeled autograft walls did not resemble either normal pulmonary or aortic walls demonstrating elastin fragmentation, decreased elastin, and increased collagen fibrosis. These histologic changes occurred in response to an increased wall stress from exposure to systemic pressure; however, the determination of remodeled autograft material properties will be necessary to understand the impact of these histologic changes on wall stress.

The Ross operation: clinical results

It is acknowledged that the Achilles' heel of the Ross operation is autograft dilatation that requires reoperation for aneurysm formation or valvular regurgitation. In clinical series using root replacement, freedom from autograft reoperation has ranged from 75% to 93% at 10 years (3,22-26). Adults who had undergone the Ross procedure required fewer reoperations than children; series without the buttressing of suture lines had higher reoperation rates; and finally variations in autograft length - particularly the length of the PA included in the root - may have also played a role in autograft longevity (5). David (27), who described autograft dilatation in its early stages (6), became a proponent of subcoronary and root inclusion techniques. Recently, David and colleagues (28) reported a 92% freedom from autograft reoperation at 15 years, for both root replacement and subcoronary/root inclusion techniques. However, these equivalent long-term results may have been skewed by the choice of root replacement for patients with a small aortic root, with previous aortic valve surgery, and in those with anomalous coronary origins, while normal and dilated aortic roots had root inclusion techniques (28). The present FE model showed a greater dilation from the baseline diameter of the PA than did the sinus regions prior to remodeling. However, due to the smaller baseline diameter of the PA, the PA and sinus diameters at systemic pressure were similar. A greater compliance of the PA than the sinus provides support to the limitation of PA length in the autograft during root replacement, as well as a potential buttressing of the STJ. However, the significant increases in autograft sinus wall stresses immediately after surgery are of concern with regards to histologic damage that may lead to elastin fragmentation and fibrosis, with aneurysmal degeneration. The present results support the concept of root inclusion or subcoronary techniques rather than root replacement techniques to use the native aortic wall for structural support.

Study limitations

The FE modeling, which was based on regional material properties, was focused primarily on the impact of pressure loading on the pulmonary root using realistic anatomic geometry, but did not include the pulmonary valve leaflets. The addition of leaflets is especially important when studying fluid flows, such

as computational fluid dynamic simulations and fluid-structure interaction simulations. However, it is believed that the simulation results regarding the extent of maximal dilation and stress are relevant. Both, the diameter and stress in the pulmonary root were greatest at peak pressure, which occurred during systole; at this point the valve leaflets were open and had a minimal impact on sinus deformation or stress. The future addition of leaflets to the model could provide a greater insight into leaflet remodeling, but would most likely not impact on the peak stress and dilation of the pulmonary root. A further limitation of the study was the inability to acquire remodeled autograft material properties from both explanted autografts and functioning autografts in order to compare differences in wall stress in vivo.

In conclusion, the highly non-linear characteristic of the pulmonary root material prevents its excessive dilation beyond the physiological range. In fact, this characteristic explains the competence of the valve following the Ross procedure, despite the significant increase in pressure. However, systemic pressure leads to an increase in wall stress by an order of magnitude, and creates stress concentrations in the sinuses. Such large increases in wall stress throughout the cardiac cycle may lead to pathologic changes of elastin fragmentation and collagen deposition, causing the remodeled autograft to be at risk of aneurysmal degeneration. Future studies using FE modeling may represent a valuable tool for evaluating new surgical techniques and devices that limit excess dilation, or reduce wall stress.

Acknowledgements

These studies were supported by the American Heart Association and Northern the California Institute for Research and Education. The authors have no financial conflicts of interest to disclose.

References

1. Stelzer P, Jones DJ, Elkins RC. Aortic root replacement with pulmonary autograft. Circulation 1989;80:III209-III213
2. Hokken RB, Takkenberg JJ, van Herwerden LA, Roelandt JR, Bogers AJ. Excessive pulmonary autograft dilatation causes important aortic regurgitation. Heart 2003;89:933-934
3. Kouchoukos NT, Masetti P, Nickerson NJ, Castner CF, Shannon WD, Davila-Roman VG. The Ross procedure: Long-term clinical and echocardiographic follow-up. Ann Thorac Surg 2004;78:773-781; discussion 781
4. Sievers HH, Hanke T, Stierle U, et al. A critical reappraisal of the Ross operation: Renaissance of the subcoronary implantation technique? Circulation 2006;114:I504-I511
5. Takkenberg JJ, Klieverik LM, Schoof PH, et al. The Ross procedure: A systematic review and meta-analysis. Circulation 2009;119:222-228
6. David TE, Omran A, Ivanov J, et al. Dilation of the pulmonary autograft after the Ross procedure. J Thorac Cardiovasc Surg 2000;119:210-220
7. Schoof PH, Takkenberg JJ, van Suylen RJ, et al. Degeneration of the pulmonary autograft: An explant study. J Thorac Cardiovasc Surg 2006;132:1426-1432
8. Grande KJ, Cochran RP, Reinhall PG, Kunzelman KS. Stress variations in the human aortic root and valve: The role of anatomic asymmetry. Ann Biomed Eng 1998;26:534-545
9. Grande-Allen KJ, Cochran RP, Reinhall PG, Kunzelman KS. Re-creation of sinuses is important for sparing the aortic valve: A finite element study. J Thorac Cardiovasc Surg 2000;119:753-763
10. Grande-Allen KJ, Cochran RP, Reinhall PG, Kunzelman KS. Finite-element analysis of aortic valve-sparing: Influence of graft shape and stiffness. IEEE Trans Biomed Eng 2001;48:647-659
11. Matthews PB, Azadani AN, Jun CS, et al. Comparison of porcine pulmonary and aortic root material properties. Ann Thorac Surg 2010;89: 1981-1988
12. Matthews PB, Kim B, Azadani AN, et al. Biomechanical perspective on the porcine pulmonary root prior to Ross remodeling. J Heart Valve Dis 2009;18:682-690
13. Siepe M, Martin J, Sarai K, Ihling C, Sommer P, Beyersdorf F. Anatomical study on the surgical technique used for xenotransplantation: Porcine hearts into humans. J Surg Res 2007;143:211-215
14. Yushkevich PA, Piven J, Hazlett HC, et al. User-guided 3D active contour segmentation of anatomical structures: Significantly improved efficiency and reliability. NeuroImage 2006;31:1116-1128
15. Carr-White GS, Afoke A, Birks EJ, et al. Aortic root characteristics of human pulmonary autografts. Circulation 2000;102:III15-III21
16. Hansen B, Menkis AH, Vesely I. Longitudinal and radial distensibility of the porcine aortic root. Ann Thorac Surg 1995;60:S384-S390
17. Lockie KJ, Butterfield M, Fisher J, Juster NP, Watterson K, Davies GA. Geometry of homograft valve leaflets: Effect of dilation of the aorta and the aortic root. Ann Thorac Surg 1993;56:125-130
18. Dagum P, Green GR, Nistal FJ, et al. Deformational dynamics of the aortic root: Modes and physiologic determinants. Circulation 1999;100:II54-II62
19. Ross D, Jackson M, Davies J. The pulmonary autograft - a permanent aortic valve. Eur J Cardiothorac

Surg 1992;6:113-116; discussion 117
20. Mookhoek A, de Heer E, Bogers AJ, Takkenberg JJ, Schoof PH. Pulmonary autograft valve explants show typical degeneration. J Thorac Cardiovasc Surg 139:1416-1419
21. Takkenberg JJ, Zondervan PE, van Herwerden LA. Progressive pulmonary autograft root dilatation and failure after Ross procedure. Ann Thorac Surg 1999;67:551-553; discussion 553-554
22. Brown JW, Ruzmetov M, Rodefeld MD, Mahomed Y, Turrentine MW. Incidence of and risk factors for pulmonary autograft dilation after Ross aortic valve replacement. Ann Thorac Surg 2007;83:1781-1787; discussion1787-1789
23. de Kerchove L, Rubay J, Pasquet A, et al. Ross operation in the adult: Long-term outcomes after root replacement and inclusion techniques. Ann Thorac Surg 2009;87:95-102
24. Elkins RC, Thompson DM, Lane MM, Elkins CC, Peyton MD. Ross operation: 16-year experience. J Thorac Cardiovasc Surg 2008;136:623-630; discussion 630, e1-e5
25. Luciani GB, Favaro A, Casali G, Santini F, Mazzucco A. Reoperations for aortic aneurysm after the Ross procedure. J Heart Valve Dis 2005;14:766-772; discussion 772-773
26. Yacoub MH, Klieverik LM, Melina G, et al. An evaluation of the Ross operation in adults. J Heart Valve Dis 2006;15:531-539
27. David TE. Ross procedure at the crossroads. Circulation 2009;119:207-209
28. David TE, Woo A, Armstrong S, Maganti M. When is the Ross operation a good option to treat aortic valve disease? J Thorac Cardiovasc Surg 139:68-73; discussion 75